Int. J. Heat Mass Transfer. Vol. 27, No. 9, pp. 1511–1523, 1984
Printed in Great Britain

0017–9310/84 $3.00 + 0.00

Effects of sound on local transport from a heated cylinder

JON A. PETERKA* and PETER D. RICHARDSON
Center for Fluid Dynamics, Division of Engineering, Brown University, Providence, RI 02912, U.S.A.

(*Received* 23 *February* 1984)

Abstract—The steady transport of heat from a horizontal circular cylinder supported in a standing transverse sound field was investigated. Experimental conditions were chosen to allow ready comparison with solutions of the momentum and energy equations. Local heat transport was studied, it being more sensitive to sound fields than overall transport. Experiments were performed with a heated cylinder in an anechoic chamber and a laser schlieren-interferometer was used to obtain local measurements of temperature gradients in the air surrounding the cylinder. Sound field intensities ranged up to 142 db. The convection was analyzed in the equations for mean motion using the Reynolds stresses generated by the sound to represent the effect of the sound field. The velocity and temperature fields of the mean motion were represented as an azimuthal series of functions of the radial coordinate, and the solutions computed at finite Grashof and streaming Reynolds numbers for conditions at the bottom stagnation region. Substantial agreement was found between experimental transport and the computed solutions for horizontal sound fields. The analysis showed that the effect of the sound field is significantly greater at the moderate Grashof numbers (O (10^3)) used in the experiments than predicted by a boundary layer analysis ($Gr \to \infty$) for otherwise similar conditions. The results support the hypothesis that effects of sound and vibrations can be accounted as the influence on the mean motion of Reynolds stresses associated with the oscillations.

DEDICATION

IN DEDICATING this work to Professor Sir Owen Saunders, FRS, we wish to pay tribute to his stimulating research in natural convection and the use of optical methods. In his paper [1] describing the optical method there was careful attention to clear presentation of the theory and notes on important details, such as the fact that the refractive index varies with the wavelength of the light; there was also comparison between theory and experiment. In a subsequent paper [2], Sir Owen applied the optical method to the study of the motion of fluid between two horizontal flat plates with the lower one heated. By collimating the light in narrow slits he showed that the fluid close to both the upper and lower plates had regular spatial variations of transport across the plates, corresponding rather well to expectations from analyses which had been made for the situation prevailing above the critical Rayleigh number. In another paper [3] he studied natural convection from a vertical flat plate to liquids, again giving emphasis to comparison between theory and experiment over a range of Prandtl numbers, and using the optical method for detection of transition in the boundary layer flow.

In preparing the present paper we have had the benefit of two specific technological advances: the laser and the digital computer. These allow optical methods and comparisons between theory and experiment to be carried further.

INTRODUCTION

Effects of sound and vibrations on fluid motion have been studied for decades. The Kundt dust tube phenomenon has been familiar to several generations of physicists. Some properties of oscillating boundary layers were known in the nineteenth century [4], and 50 years ago Schlichting [5] showed how steady streaming over a cylinder oscillating transversely to its axis could be calculated as a second-order motion driven by Reynolds stresses whose component velocities were given by the first-order (oscillatory) motion. More recently, Stuart [6, 7] has shown how this streaming motion itself has an inner and outer structure that depends upon the streaming Reynolds number. The concepts and techniques have been applied to various geometries and boundary conditions with apparent success.

Effects of sound and vibrations on convective heat transfer have been investigated quite vigorously in the past 20 years (cf. the review by Richardson [8]). At first the results suggested that some distinctive physical phenomena were involved, because overall heat transfer rates were not apparently affected at all until some critical intensity of sound or vibration was reached, beyond which a progressive effect was found, e.g. Fand and Kaye [9]. Various phenomena, including fluid instability and thermoacoustic transduction, were invoked as possible explanations but no analytical solutions were obtained to make quantitative comparisons. With further experimental investigation it became apparent that changes in local heat transfer could occur which involved both increases and decreases in the heat transfer coefficient, Jackson *et al.*

* Present address: Engineering Research Center, Colorado State University, Fort Collins, Colorado, U.S.A.

NOMENCLATURE

a	amplitude of fluid particle motion in sinusoidal oscillation
d	diameter of cylinder
F	dimensionless stream function
G	dimensionless temperature difference
Gr	Grashof number, based on cylinder radius R
Pr	Prandtl number
r	radial distance from cylinder axis
R	radius of cylinder
Re_{osc}	oscillation Reynolds number, $a\omega R/v\sqrt{2}$
Re_s	streaming Reynolds number, $a^2\omega/v$
t	time
u, v	velocity components in x, y directions
U_∞	amplitude of fluid particle velocity due to sound field which would be found at cylinder axis if the cylinder was absent
x, y	orthogonal curvilinear coordinates embedded in cylinder surface (x, tangential; y, normal) with origin at the bottom generator line.

Greek symbols

α	thermal diffusivity
β	specific buoyancy of air
γ	reciprocal of $\delta_{a.c.}$
$\delta_{a.c.}$	boundary layer thickness of oscillating flow, $\sqrt{(2v/\omega)}$
ε	dimensionless measure of acoustic streaming compared with buoyant motion, $4Re_s/Gr^{1/2}$
η	dimensionless radial distance based on the combination parameter σ
θ	temperature difference available to drive buoyant motion
ν	kinematic viscosity
σ	combination parameter for buoyant and acoustic streaming scales, equation (5)
ϕ	azimuthal angle round cylinder, origin at bottom
ψ	stream function
ω	circular frequency [rad s^{-1}].

[10], that changes in local heat transfer occur on a circular cylinder at sound intensities below that critical for changes in overall heat transfer [11], and that the direction of such changes in local heat transfer was shifted by changing the direction of the transverse sound field on the heated cylinder from horizontal to vertical [12]. Observations of this type suggested that an explanation of the heat transfer phenomena can be found through incorporation of Reynolds stress terms in the equation for mean motion, invoking no new or additional phenomenology than appropriate for simple acoustic streaming. For the cylinder with transverse oscillations, Richardson [13] calculated the heat/mass transfer associated with various asymptotic cases, and comparisons made with experimental data were encouraging. A further comparison is made possible by the data of Lowe [14]. This corresponds to the case of heat transfer by outer streaming at large streaming Reynolds numbers for data obtained with vertical vibration of a cylinder. However, such data—and more particularly those for small streaming Reynolds numbers—show departures from the asymptotic values (for $Gr/Re_{osc}^2 \to 0$) at small finite values of Gr/Re_{osc}^2. This leaves open the question of whether some additional effect is significant in determining heat transfer on a heated circular cylinder. In other words, the possibility remains that an effect additional to that of Reynolds stresses determines heat transfer at finite Grashof numbers, yet uniformly diminishes in influence as $Gr/Re_{osc}^2 \to 0$. Moreover, the departures from the asymptotic expectations are most marked in the data with the highest oscillation frequencies (sound fields); it is for such high frequency data that the possibility of thermoacoustic transduction was invoked by earlier investigators.

The issue is not resolved by seeking comparisons between experiment and analysis for geometries other than the horizontal circular cylinder in a transverse sound field. Use of other geometries in natural convection, such as vertical flat plates or vertical cylinders with vertical oscillation, have shown little effect of oscillation at all, or have given a three-dimensional flow obviously difficult to analyze. Forced convection over bodies tends to reduce the relative magnitude of the effects of oscillations, and can also introduce different phenomena [15, 16] so that comparison is not very practicable. Data exist for forced convection inside tubes used as resonators, but attempts at analysis for local details have encountered difficulties [17].

For the horizontal circular cylinder with a transverse fluid oscillation, it is possible to proceed with a boundary-layer analysis which incorporates the effects of buoyancy and of Reynolds stresses, and thus obtain solutions at finite values of Gr/Re_{osc}^2. De Vahl Davis and Richardson presented families of solutions, for the bottom stagnation point [18] and with azimuthal development around the cylinder [19]. The solutions show the same direction of shift of heat transfer with application of transverse oscillations as the experimental data, and exhibit the regions of closed streamlines in the presence of vertical oscillations as observed by Richardson [12]. The solutions are obtained under conditions applicable to large streaming Reynolds numbers, whereas most reliable experimental data are obtained with sound fields

applied, which give small streaming Reynolds numbers; and the experimental data show a roughly two-fold larger effect of oscillations than predicted by the boundary-layer analysis. The possible explanations of this discrepancy are that some additional effect is involved, or that the analysis when extended to cover small streaming Reynolds numbers will be in close agreement with the experimental data.

We sought to resolve the issue by undertaking the necessary analysis and by obtaining additional experimental data on local heat transfer; the remainder of this paper describes this investigation.

The experimental data were obtained in an anechoic chamber, using a horizontal heated cylinder with horizontal and vertical transverse standing sound fields of about 1 kHz. A relatively small temperature difference was selected for two reasons: it would minimize the distortion of the sound field by the heated air around the cylinder, and it would make measurement of local heat transfer by optical means relatively easy within the other restraints imposed physically by the apparatus. The small temperature difference led to a moderate Grashof number (roughly 10^3), and it was necessary to begin analysis by solving the simple natural convection problem for finite Grashof numbers first [20] before tackling the problem with oscillations imposed as well. The analysis was cast in the framework of the full Navier–Stokes and energy equations, rather than with boundary-layer simplifications, to correspond with the experiments.

ANALYSIS

The analysis of the effects of transverse oscillations on natural convection on a horizontal circular cylinder at moderate Grashof numbers is performed in a number of sequential steps. The analytic and experimental situations actually involve a standing transverse sound field with the cylinder supported in a velocity antinode and with the wavelength of the sound field much larger than the cylinder diameter. The flow field is obtained by solving first a linearized form of the Navier–Stokes equations for the first-order, time-dependent flow. This solution is used to generate the Reynolds stress terms for the time-independent, second-order solution. The Navier–Stokes equations for a two-dimensional, incompressible, constant property fluid are taken, where the body force terms included in the equation of mean motion are thermally induced buoyancy terms following the Boussinesq approximation. If the solution is restricted to cases where the buoyancy term is small compared to the viscous and time-dependent terms, the momentum equation after cross-differentiation and subtraction becomes

$$\nu\nabla^2\left(\frac{\partial u}{\partial y}-\frac{\partial v}{\partial x}\right)-\frac{\partial}{\partial t}\left(\frac{\partial u}{\partial y}-\frac{\partial v}{\partial x}\right)$$
$$=\frac{\partial}{\partial y}\left(u\frac{\partial u}{\partial x}+v\frac{\partial u}{\partial y}\right)-\frac{\partial}{\partial x}\left(u\frac{\partial v}{\partial x}+v\frac{\partial v}{\partial y}\right). \quad (1)$$

When the oscillation (or a.c.) boundary-layer thickness, $\delta_{a.c.}=\sqrt{(\nu/\omega)}$, is small compared to the characteristic body dimension d, the terms on the LHS are dominant. Neglect of the terms on the RHS can be shown to imply the condition $a/d \ll 1$, where a is the amplitude of oscillation. Defining the usual stream function

$$u=\frac{\partial\psi}{\partial y}, \quad -v=\frac{\partial\psi}{\partial x}$$

Rayleigh [4] has shown the solution on the LHS of equation (1) to be

$$\psi = 2U_\infty \cos x/R\left[-\frac{\cosh y/R}{\sqrt{2\gamma}}\cos\left(\omega t-\frac{\pi}{4}\right)\right.$$
$$\left.+R\sinh\frac{y}{R}\cos\omega t+\frac{e^{-\gamma y}}{\sqrt{2\gamma}}\cos\left(\omega t-\frac{\pi}{4}-\gamma y\right)\right] \quad (2)$$

where $\gamma=\sqrt{(\omega/2\nu)}$.

Following the procedure used by de Vahl Davis and Richardson [18] for the boundary-layer representation, the first-order solution can be used to generate a full solution by using equation (2) to evaluate the Reynolds stress terms of the Reynolds averaged Navier–Stokes equations. The 2-D incompressible Navier–Stokes equations in Reynolds averaged form are given by Schlichting [21]. The Reynolds stress terms evaluated from equation (2) are important only in the immediate vicinity of the wall. Their magnitude decays as $e^{-\gamma y}$ which, for the acoustic frequencies of interest, is of the order of $\delta_{a.c.} \ll d$. For this reason, a curvilinear expression of the Reynolds stress terms is acceptable. However, it has been demonstrated by Peterka and Richardson [20] that curvature effects are important in the natural convection solution at moderate Grashof numbers. Thus we transform the Reynolds averaged Navier–Stokes equations into cylindrical coordinates (r, ϕ) but retain the Reynolds stress terms in matchable curvilinear coordinates (x, y). The coordinate systems are indicated in Fig. 1. Eliminating pressure by cross-differentiation and subtraction of the ϕ and r equations, multiplication of

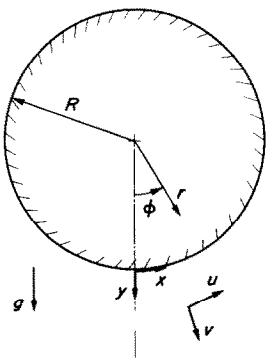

FIG. 1. Coordinate systems for analysis of natural convection on a horizontal heated isothermal circular cylinder with horizontal or vertical oscillations superimposed.

the ϕ equation by r gives, after introduction of a stream function

$$u = \frac{\partial \psi}{\partial r} \quad \text{and} \quad -v = \frac{1}{r}\frac{\partial \psi}{\partial \phi}$$

$$u\frac{\partial}{\partial \phi}(\nabla^2\psi) + rv\frac{\partial}{\partial r}(\nabla^2\psi) = r\nu\nabla^4\psi + g\beta\left(\frac{\partial \theta}{\partial \phi}\cos\phi + r\frac{\partial \theta}{\partial r}\sin\phi\right) - \left[r\frac{\partial^2\overline{u'v'}}{\partial x^2} + r\frac{\partial^2\overline{v'^2}}{\partial x\,\partial y} - r\frac{\partial^2\overline{u'^2}}{\partial x\,\partial y} - r\frac{\partial^2\overline{u'v'}}{\partial y^2} - \frac{\partial\overline{u'^2}}{\partial x} - \frac{\partial\overline{u'v'}}{\partial y}\right]. \tag{3}$$

The relations $r = y$ and $x = r\delta$ were used to perform the cross-differentiation on the Reynolds stress terms. The body force term

$$g\beta\left(\frac{\partial \theta}{\partial \phi}\cos\phi + r\frac{\partial \theta}{\partial r}\sin\phi\right)$$

where $\theta = T - T_\infty$ is the buoyancy force which couples the momentum equation to the energy equation.

The appropriate expression for the energy equation in cylindrical coordinates is

$$v\frac{\partial \theta}{\partial r} + \frac{u}{r}\frac{\partial \theta}{\partial \phi} = \alpha\left(\frac{\partial^2\theta}{\partial r^2} + \frac{1}{r}\frac{\partial \theta}{\partial r} + \frac{1}{r^2}\frac{\partial^2\phi}{\partial \phi^2}\right). \tag{4}$$

The desired solution is a simultaneous solution of equations (3) and (4) with appropriate boundary conditions and with equation (2) supplying the Reynolds stress terms in equation (3).

The partial differential equations in this form present a formidable integration problem even for a computer. In order to simplify the equations a similarity variable was derived in the manner described by Hannah [22] to describe flow against a rotating disk. The similarity variable combines the usual similarity variables for oscillating flows ($\eta = r\sqrt{(\omega/2\nu)}$) and natural convection ($\eta = r\,Gr^{1/4}/R$) into a single expression

$$\eta = r\left(\frac{\omega^2}{4\nu^2} + \frac{Gr}{R^4}\right)^{1/4} = r\sqrt{(\sigma/\nu)} \tag{5}$$

where

$$\sigma = \left(\frac{\omega^2}{4} + \frac{\nu^2\,Gr}{R^4}\right)^{1/2} \quad \text{and} \quad Gr = g\beta\Delta T R^3/\nu^2.$$

Assuming a stream function of the form

$$\psi = (\nu\sigma)^{1/2}R\phi F(\eta) \tag{6}$$

gives, after substitution into the momentum and energy equations

$$F'''' + \frac{2}{\eta}F''' - \frac{1}{\eta^2}F'' + \frac{1}{\eta^3}F' - \frac{\eta_0}{\eta^2}F'^2 - \frac{\eta_0}{\eta}F'F'' - \frac{\eta_0}{\eta} - \frac{\eta_0}{\eta^3}FF' + \frac{\eta_0}{\eta^2}FF'' + \frac{\eta_0}{\eta}FF''' + \frac{Gr}{\eta_0^4}G' \pm \frac{2Re_{osc}}{\eta_0^5}f(\eta, \eta_0, R\gamma) = 0 \tag{7}$$

and

$$G'' + \frac{1}{\eta}G' + \frac{\eta_0}{\eta}Pr\,FG' = 0$$

where

$$\eta_0 = R\sqrt{(\sigma/\nu)}, \quad G(\eta) = \frac{T - T_\infty}{T_w - T_\infty} = \frac{\theta}{T_w - T_\infty},$$

and

$$f(\eta, \eta_0, R\gamma) = \frac{\eta_0}{\eta}\left(\frac{1}{4R^2\gamma^2} - \frac{1}{2}\right) + \exp\left\{-\frac{R\gamma(\eta - \eta_0)}{\eta_0}\right. \times \left[\left(\frac{1}{2} - R^2\gamma^2 + \frac{R\gamma\eta_0}{2\eta} - \frac{3\eta_0}{4R\gamma\eta}\right)\sinh\frac{\eta - \eta_0}{\eta_0} \times \sin R\gamma\frac{\eta - \eta_0}{\eta_0} - \frac{1}{2}\left(\frac{1}{R\gamma} + \frac{\eta_0}{\eta}\right)\cosh\frac{\eta - \eta_0}{\eta_0} \times \sin R\gamma\frac{\eta - \eta_0}{\eta_0} + \frac{1}{2}\left(1 - \frac{1}{2R^2\gamma^2} + \frac{R\gamma\eta_0}{\eta} - \frac{\eta_0}{2R\gamma\eta}\right) \times \sinh\frac{\eta - \eta_0}{\eta_0}\cos R\gamma\frac{\eta - \eta_0}{\eta_0} - \left(R\gamma - \frac{\eta_0}{\eta} + \frac{\eta_0}{4R^2\gamma^2\eta}\cosh\frac{\eta - \eta_0}{\eta_0}\right)R\gamma\frac{\eta - \eta_0}{\eta_0} + \left(R\gamma - \frac{\eta_0}{2\eta}\right)e^{-R\gamma(\eta - \eta_0)/\eta_0}\right)\Bigg\}. \tag{8}$$

The formation of the body force term used the small angle approximation $\sin\phi = \phi$ and assumed $\partial\theta/\partial\phi = 0$ limiting the validity of the solution to the region of the lower stagnation point. The plus sign preceding the last term in the momentum equation is for horizontal oscillations and would be replaced by a minus sign for vertical oscillations. The appropriate boundary conditions are:

$$\begin{aligned} &\text{at} \quad \eta = \eta_0, \quad F = F' = 0, \quad G = 1 \\ &\text{at} \quad \eta \to \infty, \quad F' = F'' = G \to 0. \end{aligned} \tag{9}$$

The assumption (6) for the stream function represents the first term of an azimuthal expansion

$$\psi = (\nu\sigma)^{1/2}R[\phi F_1(\eta) + \phi^3 F_3(\eta) + \ldots]$$

and a corresponding expansion for temperature as an even function of ϕ can be made. When these expansions are substituted into the momentum equation, some additional terms arise in equation (7) involving F_3, etc. These terms are two and more orders higher than the leading terms in equation (7); incorporation of these terms would require solution of the primary differential equations for F_3 and G_2, which require the solutions F_1 and G_0 as input, and so on; thus an iterative approach to solution of the equations would be required, and solution of equation (7) as presented here represents the zeroth iterate in such a truncated series expansion [23]. The additional terms disappear in the boundary-layer limit, and become more important as Re becomes of order unity, where different azimuthal expansions can become attractive, as described by Underwood [24].

Thus, to this order in the truncated series expansion, equations (7)–(9) describe the combined effects of oscillations and natural convection in the region of the lower stagnation point on the cylinder. Even though a similarity variable was found to reduce the equations to total differential form, there is not one universal solution in terms of that similarity variable. Each of the parameters Gr, R, and ω/ν from which the similarity variable was constructed appear explicitly in the function $f(\eta, \eta_0, R\gamma)$, so that the equations must be solved for each set of values desired.

The term $f(\eta, \eta_0, R\gamma)$ in the momentum equation representing the Reynolds stress terms is shown in Fig. 2. The values of η_0, the cylinder radius, for 694 and 1294 cps are 111 and 146, respectively. Thus, the effective portion of the Reynolds stress term is seen to be within a distance of 1/10 cylinder radii from the surface and can justifiably be expressed in curvilinear form.

Equations (7) reduce to the natural convection equations for moderate Gr solved by Peterka and Richardson [19] if ω is set to zero and to the boundary-layer equations for natural convection solved by Hermann and by Chiang and Kaye [25] if, in addition, the limits of zero curvature and $Gr \to \infty$ are taken followed by one integration. The equations allow solution for isothermal streaming if Gr is set to zero. It should be noted that the boundary-layer equation of de Vahl Davis and Richardson [18] for combined oscillation and natural convection can be recovered from equations (7) by taking the limits of zero curvature and $Gr \to \infty$ and integrating once.

Equations (7) and (8) together with boundary conditions (9) constitute a sixth-order, two-point boundary-value problem. Integration of the equation set was performed numerically using a fourth-order Runge–Kutta program. The solution technique was to iterate for values of F'', F''', and G' at $r = R$ by seeking values which simultaneously make F', F'', F''', G, and G' become very close to zero at sufficiently large values of η. Because of the strongly nonlinear nature of the equations, some difficulty in converging to values of F'', F''', and G' at the wall was experienced if initial guesses of the boundary values were far from the solution values. This difficulty was overcome by varying the parameters Gr and Re_{osc} slowly from values where solutions were known to desired values, solving at each intermediate point. For cases where the velocity field extended a large distance from the cylinder, the numerical solution became unstable at large r values. This loss of stability was made worse by lowering the Grashof number and by increasing the magnitude of the vertical oscillations. The stability loss for the low Grashof numbers of interest combined with vertical oscillations was sufficient to prevent solution for vertical oscillations except at very small values of streaming Reynolds number.

Implicit in equations (7)–(9) are the solutions for natural convection at specified Grashof number, isothermal streaming at specified streaming Reynolds number, and combined natural convection and sound at specified $\varepsilon = 4Re_s/Gr^{1/2}$. The natural convection results have been reported previously. While the temperature profiles change only slightly with Grashof number, the temperature gradient at the wall, which is proportional to the heat transfer from the body, changes dramatically. The increased heat transfer coefficient at low Grashof number corresponds to relatively greater convection velocities.

Computation of solutions for effects of oscillations were confined to values of parameters appropriate for comparison with experimental conditions investigated. The computed velocity profiles for isothermal streaming are shown in Fig. 3 for an applied oscillation frequency of 694 cps. A detailed plot for $Re_s = 11$ near the origin is included to show the flow reversal near the wall as predicted by previous isothermal solutions [5]. The result indicates that, for the cylinder diameter (3/4 in.) and frequency selected, the outer streaming would be expected to be more important than the inner

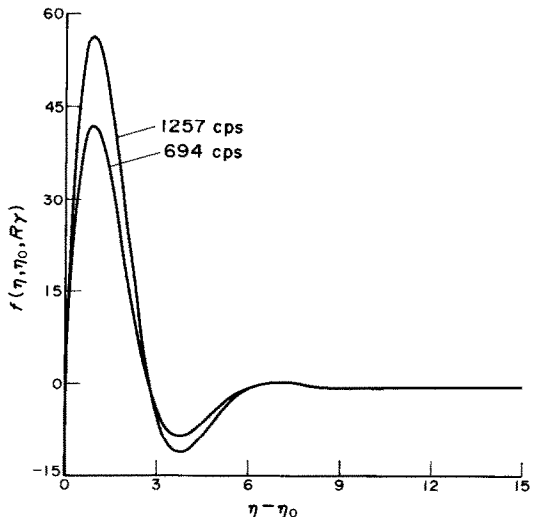

FIG. 2. Function representing the Reynolds stresses as a function of the distance from the cylinder surface.

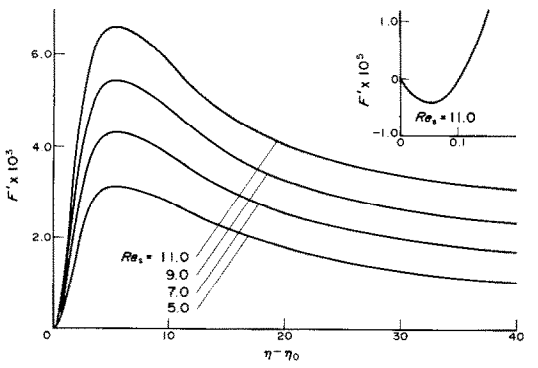

FIG. 3. Azimuthal velocity profiles for isothermal acoustic streaming around a circular cylinder at 694 cps.

streaming in its influence on heat transfer. The nondimensional variable $\eta = r\sqrt{(\omega/2\nu)}$, the usual nondimensional variable for oscillating flows, follows from setting $Gr = 0$ in equation (5).

The temperature profiles for combined natural convection and horizontal oscillations are shown in Fig. 4. The five curves represent natural convection alone ($\varepsilon = 0$) and combined natural convection and oscillation at four sound intensities. The solutions were computed for $Gr = 1380$ and 694 cps. The curves show a marked change in the shape of the temperature profile as well as in the value of the wall gradient. The thermal boundary-layer thickness can be seen to decrease with increasing oscillation amplitude as the increasing magnitude of the streaming velocity pushes it toward the cylinder. The velocity profiles corresponding to these temperature profiles are shown in Fig. 5. The velocity maximum is seen to increase and move closer to the cylinder as the oscillation amplitude is increased. The velocity profiles are consistent with the increased heat transfer evident in Fig. 4.

An approximation implicit in the first-order solution was that the body force term was negligible with respect to the time-dependent term, i.e. that the thermal boundary layer has a negligible effect on the oscillating flow. The implication is that $\partial U/\partial t \gg g\beta\theta$ or letting $\partial U/\partial t \approx U_\infty \omega$

$$\frac{U_\infty \omega}{g\beta\theta} = \frac{a\omega^2}{g\beta\theta} \gg 1$$

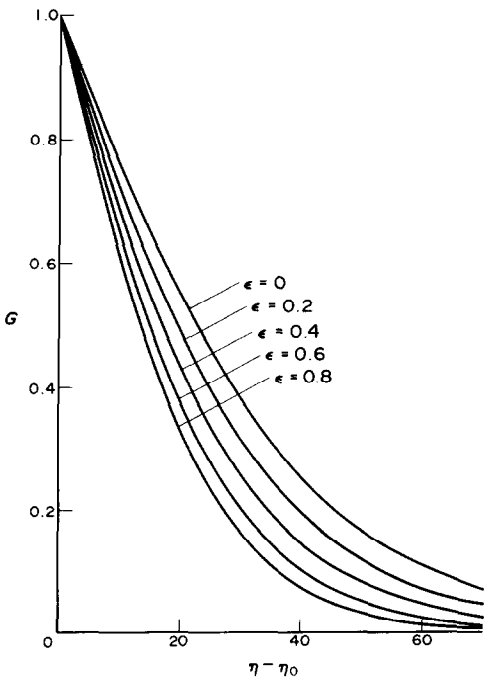

FIG. 4. Temperature profiles in the boundary layer at the bottom of a cylinder in air with $Gr = 1380$ and subjected to horizontal oscillations at 694 cps.

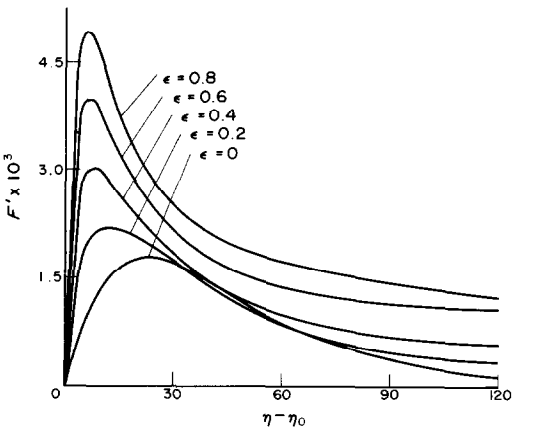

FIG. 5. Azimuthal velocity profiles in the boundary layer at the bottom of a cylinder in air with $Gr = 1380$ subjected to horizontal oscillations at 694 cps.

this is equivalent to

$$\frac{1}{128}\varepsilon^2\left(\frac{d}{a}\right)^3 \gg 1. \tag{10}$$

With typical values of $d/a > 100$, the approximation is thus valid for $\varepsilon > 0.05$, and this is appropriate for the solution used here.

A noteworthy feature of the solutions is that with the oscillation boundary layer, $(\nu/\omega)^{1/2}$, much thinner than the natural convection boundary layer, typically $R/Gr^{1/4}$, for conditions pertaining to our experiments (and for many other investigations of the same geometry) the effect of the Reynolds stresses is felt strongly at smaller values of $\eta - \eta_0$ than that associated with the maximum azimuthal velocity with natural convection alone, as is illustrated by Fig. 6. The maximum azimuthal velocity is found much closer to the cylinder when the oscillations are applied. As would be expected, the figure illustrates that the velocity profile for combined effects is not a linear addition of the two separate profiles for the independent effects and correct results would not be obtained by the simpler computational process of superposition.

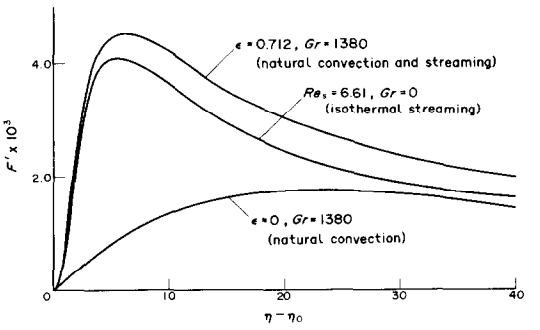

FIG. 6. Azimuthal velocity profiles associated with natural convection above, with isothermal streaming at 694 cps alone, and in the presence of both.

EXPERIMENT

The purpose of the experimental portion of the investigation was to obtain data for low Grashof numbers on the influence of a standing sound field on the heat transfer at localized positions around a cylinder. Previous experiments have measured the local heat transfer in the presence of a sound field but in every case, the Grashof number was so large that ε, the ratio of the magnitude of the sound field to that of the buoyancy field, was small enough that accurate determination of the changes occurring locally in the thermal field was difficult. The present experiment, by lowering Gr at which the tests were run, attempted to find a region in which ε was large enough to allow appreciable differences to be seen. In addition, it was anticipated that the data taken at a low Gr might provide a more useful comparison with Richardson's theory [13] developed for the asymptotic case $Gr \to 0$ than previous data taken at a higher Gr.

The experiment was performed in the anechoic chamber at Brown University. An electrically heated, silver-coated copper cylinder 3/4 in. in diameter and 18 in. long was located in the chamber with its axis horizontal. Four exponential horns were placed in pairs on either side of the cylinder and located so that a standing sound field could be established with the cylinder at a pressure node. The distance between pressure nodes of the standing sound field was an order of magnitude larger than the cylinder diameter so that, for practical purposes, the cylinder was exposed to an infinite oscillating velocity field. The horns could be placed to the side or above and below the cylinder to give horizontal or vertical fluctuations. Sound pressure levels of up to 142 db (re 0.002 dyn cm^{-2}) with uniformity of approximately 1 db were thus established about the cylinder.

A laser schlieren interferometer was used to obtain the temperature distribution in the boundary layer surrounding the cylinder. The device was developed for use in air for this experiment. Its theory of operation was demonstrated by Temple [26]. The first successful experiment was in water by Brackenridge and Gilbert [27]. A description of its first successful use and proper operational characteristics in air has been given by Brackenridge and Peterka [28] and by Brackenridge and Richardson [29].

A schematic of the schlieren interferometer is shown in Fig. 7. The schlieren interferometer differs from the Mach–Zehnder type in that it combines the test and reference beams into a single beam by allowing only a portion of the beam to be disturbed by the thermal layer. This alleviates many of the stringent alignment requirements of the two-beam systems. A small wire at the focal point of the second lens (Fig. 7) serves to subtract the principal maximum of the free field light allowing interference of the remaining disturbed and undisturbed light.

For the present experiment, the light source was a 1 mW continuous wave helium–neon laser focused

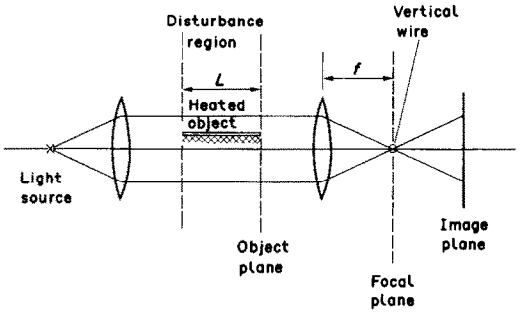

FIG. 7. Schematic diagram of a laser schlieren interferometer.

through a 4 μm hole. The purpose of the small source aperture was to allow the principal maximum of the light in the focal plane to be sufficiently small to meet the operational criteria of the instrument as set forth by Temple and as evaluated experimentally by Brackenridge and Peterka [28]. The laser source was necessary to obtain sufficient light intensity at the image plane. Collimation and refocusing of the beam was accomplished with 48 in. focal-length parabolic mirrors. A 9 μm wire was located at the focal point of the second mirror and its position was adjusted by means of a microscope slide-mount traversing mechanism. A single lens reflex camera with a special lens capable of focusing beyond infinity was used as the image plane cum data recorder and was focused on the object plane. All optics of the schlieren interferometer were located external to the anechoic chamber with the collimated beam passing through the chamber parallel to the test cylinder axis via two optical glass windows. Complete alignment of the optical system could be performed in about 2 h while day-to-day fine realignment required about 5 min.

The experiments consisted of heating the cylinder in the standing sound field with either horizontal or vertical oscillations of various intensities. The interference pattern produced by the optical system representing the 2-D temperature distribution about the cylinder was photographed and preserved for data reduction. Total heat transfer measurements were made by energy balance for some cases for comparison purposes. The temperature difference between the cylinder and ambient air was obtained from thermocouples imbedded in the cylinder and a reference thermocouple placed in the chamber. Because of the difficulties associated with measuring very small steady velocities in the presence of a larger oscillating component and because the primary interest of the study was the heat transfer, no attempt was made to obtain velocity measurements directly.

Interpretation of the fringe pattern developed by the schlieren interferometer is the same as for the Mach–Zehnder type. Measurement of fringe location from a photographic enlargement of the 35 mm negative allowed the spatial distribution of temperature to be calculated. Graphical differentiation was used to

obtain heat transfer from the temperature distribution.

A typical series of measurements of fringe patterns for horizontal oscillations and constant Grashof number but varying sound intensity are shown in Fig. 8. The supporting wires, heater wires and thermocouple leads can be seen in the photographs. The first view is for natural convection only. The outer streaming, the dominant streaming velocity seen in the theoretical solution, is toward the cylinder on the top and bottom and away from the cylinder at the sides when a horizontal standing sound field is applied. As the sound intensity is increased, the boundary-layer thickness becomes progressively thinner at the bottom and thicker at the sides. The wake becomes wider and finally is split into two clearly defined plumes as the flow separates from the surface at the sides near the $\phi = 90°$ position. These effects are consistent with and induced by the streaming velocity. The fringe pattern above the cylinder in the last two photographs shows a certain ambiguity. There are two reasons for this. Once the flow had separated into two plumes, the flow above the cylinder was quite unsteady with a vortex action re-

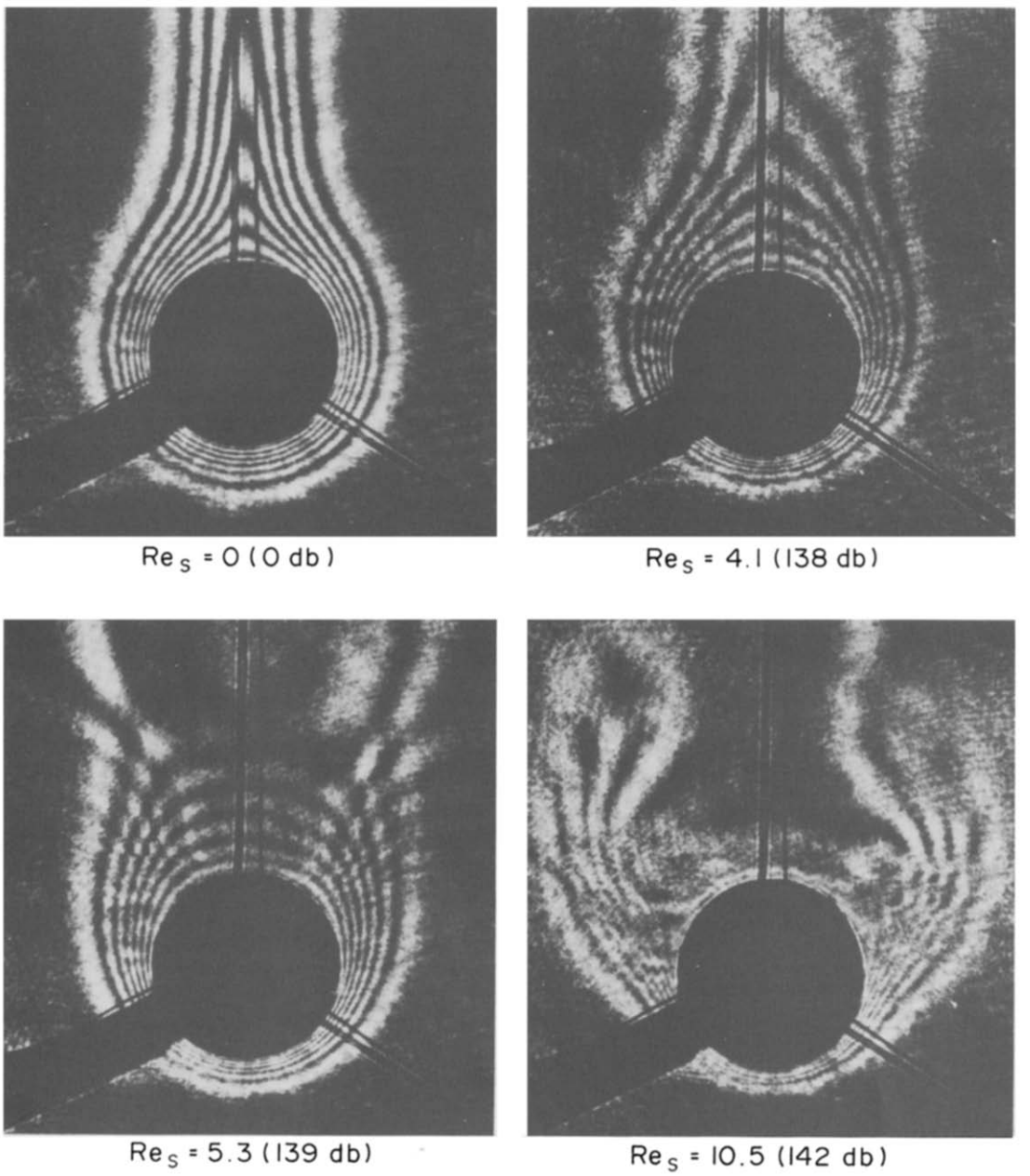

FIG. 8. Effect of a horizontal standing sound field on the boundary layer around a horizontal heated circular cylinder. The fringes in the photographs correspond to isotherms in the air around the cylinder, with the temperature difference between adjacent isotherms being constant.

circulating air from the plume back into the downward streaming area directly above the cylinder. In addition, for sound levels near 140 db where the distinct separation of the plume into two regions occurs, slight variations in sound intensity along the cylinder, even a 1 db variation, caused a nonuniform plume movement along the top of the cylinder. This condition is apparent in the third photograph in which the wake had split at the center of the 18 in. length of cylinder but not at the end where the sound pressure level was about 1 db lower.

It is apparent that the heat transfer increases over the lower portion of the cylinder as oscillations are increased. Initially, the heat transfer decreases over the top portion of the cylinder as the width of the wake is increased then increases when the splitting of the wake allows cooler air to hit the top region. The net effect on total heat transfer is that virtually no net change is evident up to the 140 db sound level, with increases and decreases almost balancing. Above 140 db, the total heat transfer rises rapidly as was noted by Fand and Kaye [9] as both the top and bottom of the cylinder are

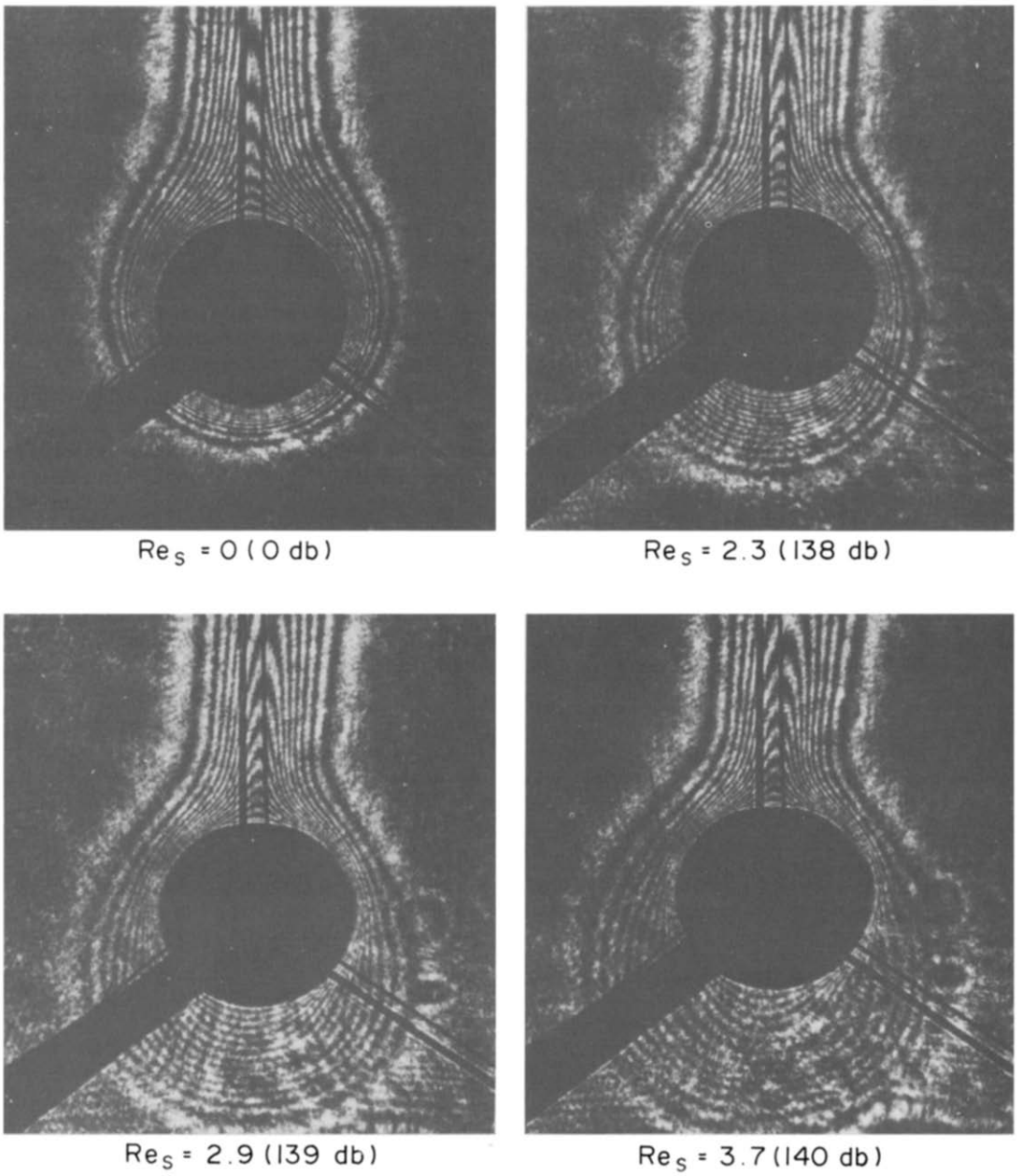

FIG. 9. Effect of a vertical standing sound field on the boundary layer around a horizontal heated circular cylinder. The fringes in the photographs correspond to isotherms in the air around the cylinder, with the temperature difference between adjacent isotherms being constant.

affected in the same way. The vortex pattern they reported for sound pressure levels above 140 db and designated as 'thermoacoustic streaming' can be seen in the last photograph. It appears that the air in the boundary layer close to the cylinder has its motion controlled dominantly by the Reynolds stresses, and thus at higher intensities the flow follows the general pattern of acoustic streaming, with radial outflow away from the cylinder at the sides; however, the Reynolds stresses fade away as distance increases from the surface and the air which has been pushed away from the cylinder then responds dominantly to the buoyant body force which it continues to experience, leading to an upward swerve of the heated air. The downflow towards the top of the cylinder, also associated with the streaming motion, appears to entrain some of the rising heated air and the combination of upflow and downflow creates a vortex-like motion above the cylinder. The 'critical' sound pressure level of 140 db identified by Fand and Kaye as the threshold level of acoustic influence on heat transfer is in fact the level at which *net* heat transfer effects become large, whereas significant heat transfer changes occur locally for much lower sound pressure levels.

A typical set of measurements of fringe patterns for constant Grashof number and varying vertical oscillation amplitude is shown in Fig. 9. The streaming velocity for this case is toward the cylinder at the sides and away from the cylinder at the top and bottom. The thermal boundary layer can be seen to respond to the streaming velocity. The heat transfer decreases greatly at the lower stagnation point and increases at the cylinder shoulders. The net result is a decrease in net heat transfer. The movement of the thermal driving forces away from the cylinder at the lower stagnation point caused a major obstacle in the analysis: the distance that integration had to be taken to match the outer boundary condition at an effective infinity increased greatly and the resulting instability of the computations prevented satisfactory solutions except at small oscillation amplitudes.

A comparison is made in Fig. 10 of the temperature distributions from theory and experiment at the lower stagnation point for horizontal oscillations. The theory is seen to agree very well with the experimental data. The fringes in the immediate vicinity of the wall were disturbed by the Fresnel diffraction pattern so that data in that region was not obtained. In Fig. 11, the local Nusselt number at the lower stagnation point is shown. The solid line is the present theoretical solution for horizontal oscillations and the dashed lines are from the theoretical solution of de Vahl Davis and Richardson. The experimental data and the theory of de Vahl Davis and Richardson were obtained concurrently with the anticipation that the boundary layer representation would be sufficient to describe the experimental results. The disparity in the results spurred the present analysis to find the proper analytical representation for the experimental conditions. The agreement between the present analysis and the experiment is as good as the experimental determination of heat transfer allows.

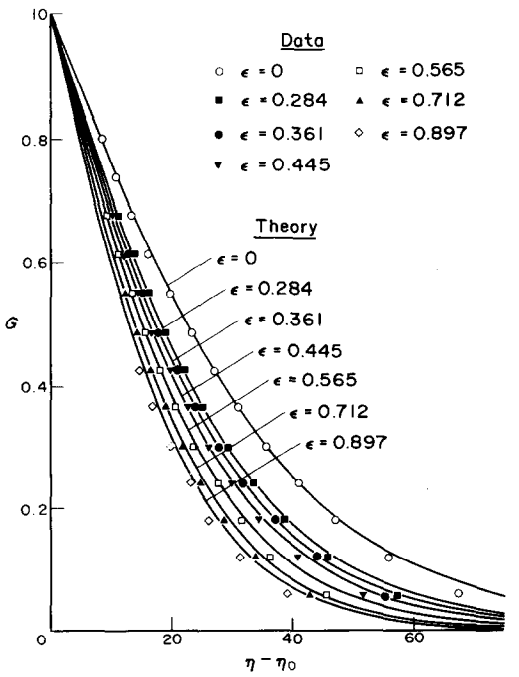

FIG. 10. Temperature distributions in the boundary layer at the bottom stagnation point of a heated horizontal circular cylinder subjected to a transverse horizontal standing sound field: comparison of analysis and experiment.

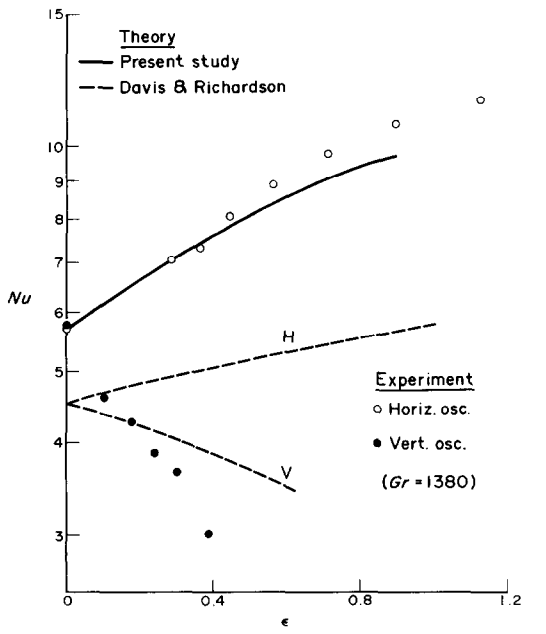

FIG. 11. Variation of local Nusselt number at the bottom of a heated horizontal circular cylinder subjected to a horizontal or a vertical sound field.

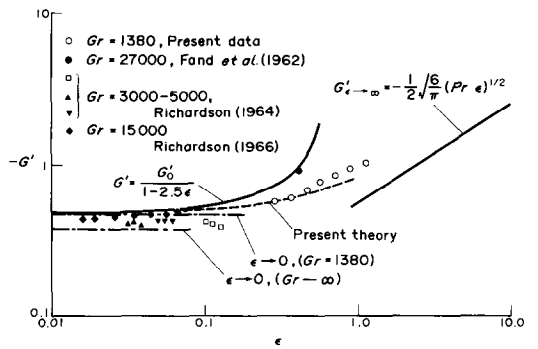

FIG. 12. Relationship of present analysis and experimental data to asymptotic analyses (heat transfer by natural convection or by acoustic streaming alone).

Figure 12 shows the relationship that the present theory and experiment have to theories for the asymptotic solutions and aids in the determination of the range of validity of the limiting theories.

DISCUSSION

The experiments and analysis reported here were carried out with the objective of establishing whether effects of sound and vibrations on heat transfer could be accounted for by the influence of Reynolds stresses associated with the oscillations when examined on a local basis. An experimental arrangement that is convenient for both accurate measurement of local heat transfer and formulation of the analytic problem was used. The apparatus provided not only extensive local information on the effects of sound on heat transfer, but also shows graphically the modification of the boundary-layer region around the whole perimeter of the horizontal circular cylinder. The greatest difficulties in effecting the comparison lay in the computational process associated with the analysis: obtaining convergent solutions with three unknown boundary values at the cylinder surface were (computer) time consuming. In view of the considerably greater difficulty that arose in computation for vertical oscillations, resources were concentrated largely on computation for effects of horizontal oscillations.

The agreement between the experiments and the computations for horizontal oscillations (Fig. 11) is substantial, and supports the hypothesis that the effect of sound and vibrations can be accounted for by the influence of Reynolds stresses associated with the oscillations. Circumstances where this applies should not be confused with those where instability effects arise (e.g. Peterka and Richardson [15]). One noteworthy difference between effects driven by Reynolds stresses, as described here, and those effects involving instability interactions is that the effect of change of frequency is much smoother with the former. A change of frequency, with all other variables held constant, will have a change of the parameters σ and ε associated with it but the set of solutions is smoothly continuous with change of these parameters. On the other hand, effects involving instability interactions occur only over a narrow waveband (and perhaps at a harmonic or two of the principal frequency).

The interferographs demonstrate clearly a feature found in previous experiments: local changes in heat transfer around a cylinder differ in direction at different azimuthal locations and nearly match in magnitude, so that effects of oscillations are much less noticeable on overall heat transfer than on local heat transfer. This serves to re-emphasize the value of local measurements when attempts are being made to understand the physical basis of specific phenomena.

The difficulties in carrying out numerical analysis for the particular circumstances of the experiments provide a somewhat chastening experience. To perform the corresponding computations for related experimental data available in the literature would be expensive in computer time without necessarily providing a sensitive examination of the comparison between data and analysis. The range of values of the pertinent parameters which can be achieved in experimental circumstances emphasize the usefulness of a set of asymptotic analyses. Generalization of the question of quantitative effects of oscillations to a wide variety of body shapes—ellipses, inclined plates, spheroids, and so on—with ranges of parameters applicable to them similar to those arising for the circular cylinder would present a formidable computational problem.

The interferographs for the effects of vertical oscillations present a remarkable instance of boundary layer thickening in the bottom stagnation region. Analysis and visual observation indicate that a pair of vortices—that is to say, regions with closed streamlines—exist within the thickened boundary layer. Over the range of streaming Reynolds numbers used with vertical oscillations (up to 3.7) no instability of this closed streamline region was observed, but higher intensities of oscillation might have led to it; instability of this region has been reported with vertical oscillations of this order of intensity but on a cylinder with higher Grashof number [12]. Instability of this flow regime could be of practical importance for it might be accompanied by a significant increase in the overall heat transfer.

The influence of Reynolds stresses is seen in the time-mean momentum equation as terms giving finite spatial gradients of the Reynolds stresses. Such spatial gradients arise when the surface of a body is not a flat plane aligned with its surface in the direction of the imposed oscillations, or when the wavelength of the oscillations is small compared with the extent of the surface even if it is flat and parallel to the direction of the oscillations. Such spatial gradients can exist in many surface configurations, and effects of the sort described here for one geometry can be expected to occur with many others.

Acknowledgements—The experimental measurements were performed in connection with part of the research program of

heat transfer in unsteady flows of the Aeronautical Research Office of the U.S. Air Force. The computations were supported by NSF Grant GP-4825.

REFERENCES

1. O. A. Saunders, M. Fishenden and H. D. Mansion, Some measurements of convection by an optical method, *Engineering* **139,** 483–485 (1935).
2. R. J. Schmidt and O. A. Saunders, On the motion of a fluid heated from below, *Proc. R. Soc.* **A165,** 216–228 (1938).
3. O. A. Saunders, Natural convection in liquids, *Proc. R. Soc.* **A172,** 55–71 (1939).
4. Lord Rayleigh, On the circulation of air observed in Kundt's tubes, and on some allied acoustical problems, *Phil. Trans. R. Soc.* **A175,** 1 (1884).
5. H. Schlichting, Berechnung ebener periodischer Grenzschichtstromungen, *Phys. Z.* **33,** 327–335 (1932).
6. J. T. Stuart, Unsteady boundary layers, in *Laminar Boundary Layers* (edited by L. Rosenhead), Chap. VII. Oxford University Press, Oxford (1963).
7. J. T. Stuart, Double boundary layers in oscillatory viscous flow, *J. Fluid Mech.* **24,** 673–687 (1966).
8. P. D. Richardson, Effects of sound and vibration on heat transfer, *Appl. Mech. Rev.* **20,** 201–217 (1967).
9. R. M. Fand and J. Kaye, The influence of sound on free convection from a horizontal cylinder, *Trans. Am. Soc. Mech. Engrs*, Series C, *J. Heat Transfer* **83,** 133–143 (1961).
10. T. W. Jackson, K. R. Purdy and C. C. Oliver, The effects of resonant acoustic vibrations on the Nusselt numbers for a constant temperature horizontal tube, *Int. Dev. Heat Transfer*, Part II, 483–489 (1961).
11. P. D. Richardson, Effect of sound upon local heat transfer from a cylinder, *J. Acoust. Soc. Am.* **36,** 2323–2327 (1964).
12. P. D. Richardson, Local details of the influence of a vertical sound field on heat transfer from a circular cylinder, *Proc. 3rd Int. Heat Transfer Conf.*, Vol. 3, pp. 71–77 (1966).
13. P. D. Richardson, Heat transfer from a circular cylinder by acoustic streaming, *J. Fluid Mech.* **30,** 337–355 (1967).
14. P. D. Richardson and K. Tanishita, Analysis of Lowe's measurements of effects of vibration on heat transfer, *Int. J. Heat Mass Transfer* **17,** 1118–1119 (1974).
15. J. A. Peterka and P. D. Richardson, Effects of sound on separated flows, *J. Fluid Mech.* **37,** 265–287 (1969).
16. S. Okamoto, T. Hirose and T. Adachi, The effect of sound on the vortex shedding from a circular cylinder, *Bull. Jap. Soc. Mech. Engrs* **24,** 45–53 (1981).
17. T. W. Jackson and K. R. Purdy, Resonating pulsating flow and convective heat transfer, *Trans. Am. Soc. Mech. Engrs*, Series C, *J. Heat Transfer* **87,** 507–512 (1965).
18. G. de Vahl Davis and P. D. Richardson, Natural convection in a sound field giving a large streaming Reynolds numbers, *Int. J. Heat Mass Transfer* **16,** 1245–1265 (1973).
19. G. de Vahl Davis and P. D. Richardson, Interaction between a sound field and natural convection on a horizontal cylinder, *Proc. IUTAM Symp. on Unsteady Boundary Layers*, Vol. 2, pp. 1584–1652. Laval University Press (1972).
20. J. A. Peterka and P. D. Richardson, Natural convection from a horizontal cylinder at moderate Grashof numbers, *Int. J. Heat Mass Transfer* **12,** 749–752 (1969).
21. H. Schlichting, *Boundary Layer Theory*. McGraw-Hill, New York (1968).
22. D. M. Hannah, Aero. Res. Coun. Rep. & Mem. 2772 (1947).
23. D. A. Saville and S. W. Churchill, Laminar free convection in boundary layers near horizontal cylinders and vertical axisymmetric bodies, *J. Fluid Mech.* **29,** 391–399 (1967).
24. R. L. Underwood, Calculation of incompressible flow past a circular cylinder at moderate Reynolds numbers, *J. Fluid Mech.* **37,** 95–114 (1969).
25. T. Chiang and J. Kaye, On laminar free convection from a horizontal cylinder, *Proc. 4th U.S. Natl. Congr. Appl. Mech.*, Vol. 2, pp. 1213–1219 (1962).
26. E. G. Temple, Quantitative measurement of gas density by means of light interference in a Schlieren system, *J. Opt. Soc. Am.* **47,** 91–100 (1957).
27. J. B. Brackenridge and W. P. Gilbert, Schlieren interferometry. An optical method for determining temperature and velocity distributions in liquids, *Appl. Optics* **4,** 819–821 (1965).
28. J. B. Brackenridge and J. A. Peterka, Criteria for quantitative Schlieren interferometry, *Appl. Optics* **6,** 731–735 (1967).
29. J. B. Brackenridge and P. D. Richardson, The Schlieren interferometer, Brown Univ. Div. Engng Rept. AF 1754/2 (1967).

EFFETS DU SON SUR LE TRANSFERT LOCAL D'UN CYLINDRE CHAUFFE

Résumé—On étudie le transfert thermique stationnaire d'un cylindre circulaire horizontal, avec un champ sonore transversal. Des conditions expérimentales sont choisies pour permettre une comparaison valable avec des solutions des équations de quantité de mouvement et d'énergie. On constate que le transfert local thermique est plus sensible aux champs sonores que le transfert global. Des expériences faites avec un cylindre chauffé dans une chambre sourde et avec un interféromètre laser permettent la mesure locale des gradients de température dans l'air autour du cylindre. Les intensités du champ sonore atteignent 142 db. La convection est analysée dans les équations du mouvement moyen utilisant les contraintes de Reynolds générées par le son, pour représenter l'effet du champ sonore. Les champs de vitesse et de température du mouvement moyen sont représentés avec une série azimutale de fonctions de la coordonnée radiale et les solutions calculées à des nombres de Grashof et de Reynolds finis pour des conditions de la région du point d'arrêt inférieur. Un accord sensible entre le transfert expérimental et les solutions calculées est trouvé pour les champs sonores horizontaux. L'analyse montre que l'effet du champ sonore est significativement plus grand aux nombres de Grashof modérés ($O(10^3)$) que prévu par une analyse de couche limite ($Gr \to \infty$) pour des conditions similaires. Les résultats soutiennent l'hypothèse que les effets du son et des vibrations peuvent être considérés comme l'influence des contraintes de Reynolds sur le mouvement moyen.

DER EINFLUSS VON SCHALL AUF DIE LOKALEN TRANSPORTPHÄNOMENE AN EINEM BEHEIZTEN ZYLINDER

Zusammenfassung—Der stationäre Wärmetransport an einem horizontalen Kreiszylinder in einem stehenden transversalen Schallfeld wurde untersucht. Die experimentellen Bedingungen wurden so gewählt, daß Vergleich mit vorhandenen Lösungen von Impuls- und Energiegleichung angestellt werden konnte. Der lokale Wärmetransport wurde deshalb untersucht, weil dieser empfindlicher von Schallfeldern abhängig ist als der mittlere Wärmetransport. Die Versuche wurden mit einem beheizten Zylinder in einer schalltoten Kammer durchgeführt. Ein Laser-Schliereninterferometer wurde zu Messungen der lokalen Temperaturgradienten in der den Zylinder umgebenden Luft benutzt. Die Intensität des Schallfeldes reichte bis 142 db. Die Konvektion wurde mit den Gleichungen für die mittlere Bewegung untersucht, wobei die durch den Schall erzeugten Reynolds-Spannungen benutzt wurden, um den Einfluß des Schallfeldes zu berücksichtigen. Die Geschwindigkeits- und Temperaturfelder für die mittlere Bewegung wurden durch eine azimutale Reihe von Funktionen der radialen Koordinate dargestellt und Lösungen bei kleinen Grashof- und Reynolds-Zahlen für Bedingungen des unteren Staubereiches berechnet. Es wurde eine grundsätzliche Übereinstimmung zwischen den experimentellen Ergebnissen und den berechneten Lösungen für ein horizontales Schallfeld gefunden. Die Untersuchung zeigte, daß der Einfluß des Schallfeldes für mäßige Grashof-Zahlen—wie bei den Versuchen—signifikant größer ist als wenn er durch eine Grenzschichtuntersuchung für ($Gr \to \infty$) bei sonst ähnlichen Bedingungen erhalten wurde. Die Ergebnisse stützen die Hypothese, daß von Schall und Vibration ausgehende Effekte durch den Einfluß der von den Oszillationen verursachten Reynolds-Spannungen auf die mittlere Bewegung erklärt werden können.

ВЛИЯНИЕ ЗВУКА НА ЛОКАЛЬНЫЙ ПЕРЕНОС ТЕПЛА ОТ НАГРЕТОГО ЦИЛИНДРА

Аннотация—Проведено исследование стационарного переноса тепла от горизонтального круглого цилиндра, находящегося в стоячем поперечном звуковом поле. Экспериментальные условия выбирались таким образом, чтобы можно было проводить непосредственные сравнения с решениями уравнений импульса и энергии. Исследовался локальный перенос тепла, который более подвержен воздействию звукового поля, чем суммарный. Эксперименты проводились с нагретым цилиндром, помещенным в глухую камеру, с использованием лазерного теневого интерферометра для локальных измерений градиентов температур в окружающем цилиндр воздухе. Интенсивность звукового поля достигала 142 дб. С помощью генерируемых звуком напряжений Рейнольдса проводился анализ конвекции, учитываемой в уравнениях усредненного движения, с целью выяснения влияния звукового поля. Поля скорости и температуры усредненного движения представлены в виде азимутального ряда функций радиальной координаты, а также в виде решений, полученных при конечных значениях числа Грасгофа и числа Рейнольдса для потока для условий в критической области в нижней части цилиндра. Получено хорошее совпадение между экспериментальными и расчетными данными для горизонтальных звуковых полей. Анализ показал, что звуковое поле оказывает гораздо более сильное влияние на теплоперенос при умеренных значениях числа Грасгофа (порядка 10^3), используемых в экспериментах, чем это следует из расчетов по теории пограничного слоя ($Gr \to \infty$) при прочих равных условиях. Результаты подтверждают предположение о том, что влияние звукового поля и вибрации можно рассматривать как влияние на усредненное движение рейнольдсовских напряжений, вызванных колебаниями.